# INVESTIGATION OF BAMBOO NODES INTERNAL STRUCTURE WITH X-RAY MICRO-CT IMAGING

*Judith Gouin[a,b], Pascal Turberg[b,c], Anastasios P. Vassilopoulos[a]*

a: Composite Construction Laboratory (CCLab), Ecole Polytechnique Fédérale de Lausanne (EPFL), 1015 Lausanne, Switzerland – judith.gouin@epfl.ch
b: Plant Ecology Research laboratory (PERL), Ecole Polytechnique Fédérale de Lausanne (EPFL), 1015 Lausanne, Switzerland
c: WSL Swiss Federal Institute for Forest, Snow and Landscape Research, Site Lausanne, Switzerland

**Abstract:** *This study presents the 3D characterization of the nodal region of an Arundinaria amabilis bamboo using X-ray micro-computed tomography imaging (µCT). The complex pattern of vascular bundles across the node was identified, and the sample was characterized regarding the relative volumes of parenchyma and sclerenchyma tissues. The results show that the node witnesses the development of radial and tangential vascular bundles, forming a net-like pattern. Some specific nodal structures ("splitting bundles") were also identified: regularly distributed around the culm, they split below the diaphragm between bundles crossing radially into the diaphragm and others deviating to the outer side of the culm. Finally, the volumetric fraction of lignified sclerenchyma tissue reaches a minimum at the location of the node. In addition, the µCT technique was used to build a discretized model of an internodal part of the bamboo sample, thus allowing to recreate the real 3D structure of the composite material and showcasing the potential of µCT imaging for finite element analysis.*

**Keywords:** Bamboo node; X-ray microtomography; 3D reconstruction; Vascular bundles; Finite-element model

## 1. Introduction

Bamboo is a sustainable, fast-growing and resistant material used in the construction industry in recent years, as an environmentally friendly alternative to more traditional and polluting construction materials. A bamboo culm is composed of an alternation of hollow internodes and solid nodes [1] and consists of vascular bundles embedded in parenchyma ground tissue. Bamboo is considered a natural composite, and its morphological structure directly influences its mechanical properties. The vascular bundles are responsible for the transport of water and nutrients within the culm and are themselves composed of xylem and phloem vessels surrounded by protective fiber sheaths made of sclerenchyma tissue. The sclerenchyma fibers are dense and provide strength and stiffness to the bamboo culm [2] while the parenchyma ground tissue behaves like a foam and distributes the local stresses to the whole structure as a matrix [3,4].

The structure of internodes is today well understood; the vascular bundles are longitudinally arranged in internodes and their distribution follows a radial density gradient. The morphological structure of bamboo nodes – controlling the mechanical properties - is however more complex and has been less studied. Research on bamboo nodes began in the 1960s [6], relying mainly on optical microscopy. Using enlarged images of longitudinal and transverse

 

sections, [7] studied the anatomical characteristics of vascular bundles in bamboo nodes, while [8] reconstructed by hand the complex 3D structure of a node, showing that bamboo nodes witness an intensive fusion and separation of conducting cells as well as vascular bundles deviating from their longitudinal path and passing horizontally through the diaphragm.

2D visualization methods remain limited since they require complex and sometimes damaging preparations of the samples. In recent years, several studies have turned to the high-resolution and non-invasive technique of X-ray microtomography (µCT) to better understand the internal structure of bamboo nodes through 3D reconstruction [10-14]. However, among those, only [14] investigated the structure of a simple node (without any type of branching) through 3D reconstruction which provided a general view of the fibers' connectivity but didn't discuss the effect the fibers have on the node's performance. Indeed, there is to this day no consensus on the mechanical properties of bamboo nodes and the research on this topic remains quite sparse and often contradictory, nodes being seen either as weak points in the culm or helping to strengthen it [9, 15-16].

The main goal of this work is to isolate the path of individual fibers in a bamboo node to better understand the behavior of the vascular bundles in the node and how it affects the mechanical properties of bamboo nodes. With this view in mind, this study is also investigating the potential of µCT imaging for building a finite-element model of the node. Such model based on the real 3-dimensional geometry of the node would indeed allow to perform numerical simulations that could be of critical interest for the understanding of the node behavior. An FE model of a node is built following a simple procedure based on an automatic threshold.

## 2. Materials and methods

### 2.1 Material

Samples of *Arundinaria amabilis* bamboo were purchased from www.bambushandel-condam.de. A section of the culm of 21 mm in height, with an external diameter of 26 mm and internal diameter of 17mm, was selected for µCT scanning. The node was positioned at the center of the scanned sample.

### 2.2 X-ray computed microtomography

The µCT imaging technique is based on the attenuation of the X-ray radiation by the scanned material. It thus allows to detect materials that attenuate the radiations differently. In the case of bamboo, dense fibers tend to attenuate a lot the X-rays, while the softer and more porous parenchyma attenuates less. As for the conducting vessels, they do not attenuate at all X-rays. µCT imaging therefore allows to detect the three main components of a bamboo culm: parenchyma, fibers and conducting vessels. The sample was scanned using an Ultratom X-ray imaging system from RX solutions. The following scan parameters were used: X-ray source voltage of 45 kV, current of 311 µA, and averaging over 6 pictures. The images were acquired at a rate of 2.5 pictures/second and a total of 1632 projections were used. A resulting voxel size of 0.0143 µm was obtained.

### 2.3 Image processing

Images were processed and analyzed using the AVIZO 3D software (2021.1 version). The slices were combined and reconstructed from the projections with a non-iterative filtered backprojection algorithm and exported as a stack of TIFF images. A total of 1509 slices was obtained. The original TIFF stack was denoised using the non-local means denoising filter of

 

AVIZO 3D. The automatic threshold function of AVIZO 3D was then used to segment the different tissues from one another: fibers, parenchyma and conducting vessels (Figure 2). The volumetric content of the different components was then computed for the whole sample as well as for each transverse slice.

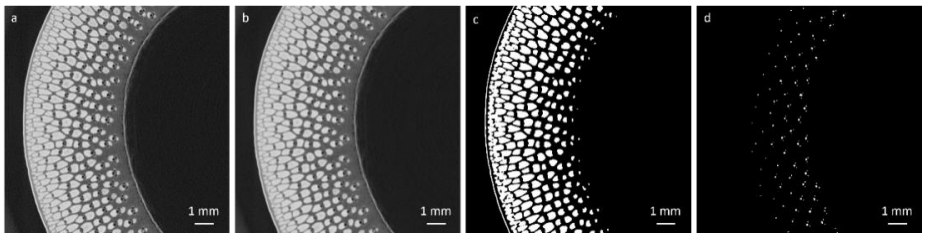


*Figure 2. Image processing of the µCT stack. (a) Detail of an original transverse µCT section. Color scale: densest and most attenuating materials (fibers) in white to least attenuating materials (voids) in black. (b) After denoising with a non-local means filter. (c) Binary mask of the fibers after segmentation. (d) Binary mask of the conducting vessels after segmentation.*

### 2.4 Finite-element model

Once the segmentation of the different components of the culm was performed, an attempt was made at meshing the structure. The goal was to obtain a finite-element model that could be exported to ABAQUS software for further numerical simulations. To ease the meshing, the structure was simplified by considering only the parenchyma and the fibers: the conducting vessels, which represent no more than a few percent of the culm in terms of volume, were included in the parenchyma segmentation. Two approaches were followed to develop the finite-element model. The first one was based on the generation of a surface mesh using the AVIZO 3D *"Generate surface"* function. The generated surface was then exported as an .STL file into the open-source software Meshmixer, where the mesh was repaired and simplified. Finally, the open-source software Gmsh was used to compute the final solid mesh from the surface mesh. An alternative approach was also implemented using the X-Wind meshing module of AVIZO 3D, which allows to directly compute a solid mesh based on a given segmentation.

## 3. Results and discussions

### 3.1 Morphological analysis of the node

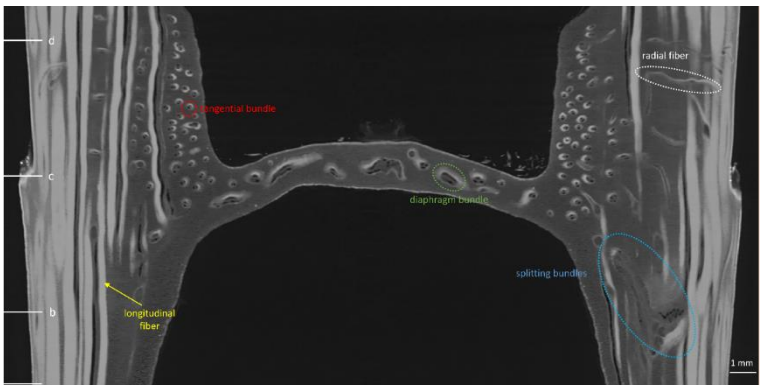


*Figure 3. Longitudinal view of the node and identification of different types of vascular bundles.*

The general morphology of an *Arundinaria amabilis* bamboo node can be seen in Figure 3. On the transverse sections (Fig. 4 and 5) the different components of the culm can be well

 

distinguished: the parenchyma and the vascular bundles consisting of the sclerenchyma fibers and the conducting vessels. The morphological characteristics of fibers and vascular bundles in the node can be identified on the longitudinal and transverse section views of Figures 3 to 5.

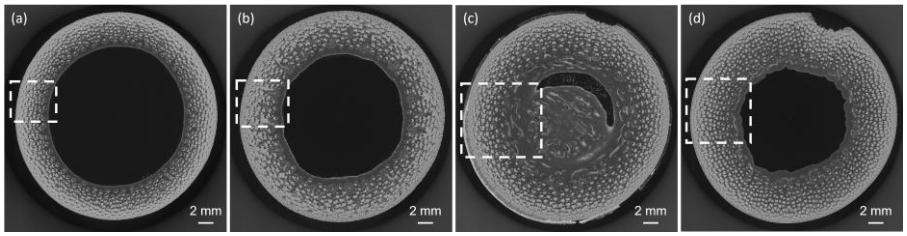


*Figure 4. Transverse views at different locations of the culm. (a) at the bottom. (b) below the diaphragm. (c) at the sheath scar and diaphragm position. (d) above the diaphragm.*

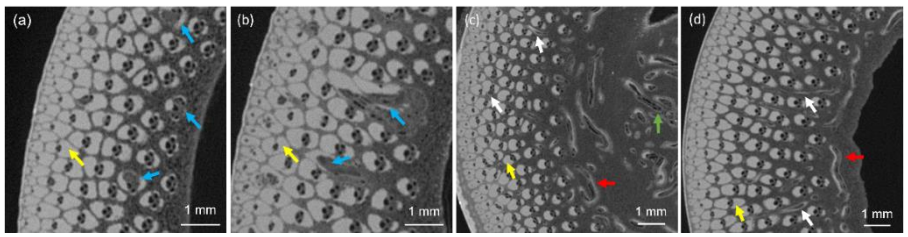


*Figure 5. (a to d) Close-up of the transverse slices of Fig. 4. Longitudinal fibers (yellow arrows), splitting bundles (blue arrows), tangential bundles (red arrows), radial fibers (white arrows), diaphragm bundle (green arrow).*

At the bottom of the node (Fig. 5a) all the fibers have a longitudinal orientation. Closer to the node, the thickness of the culm increases, and the vascular bundles tend to lose completely their lateral fiber sheaths, while the two polar sheaths of the bundles increase in size and become rounder, as had already been noticed by [7] and [9]. Some peculiar layout also begins to appear, called "splitting bundles" in this manuscript. The "splitting bundles" are originally located on the inner layer of the culm and regularly distributed on its circumference (Fig. 5a, blue arrows). They first begin to dilate (Fig. 5a, blue arrows), before splitting below the diaphragm into several bundles (Fig. 5b, blue arrows): some will deviate radially of a few millimeters towards the outer side of the culm before regaining a longitudinal orientation, while another bundle will develop towards the center of the culm and cross into the diaphragm (Fig. 3). That specific type of "splitting bundles" had not been analyzed by [14] but can however be detected on the µCT node images shown in that paper. Those bundles seem to be a critical element for the transverse transport of water and nutrients in the culm.

The bundles that cross into the diaphragm mostly have a horizontal orientation (Fig. 3 and 5, green arrows). Unlike the longitudinal vascular bundles of the culm which have large fiber sheaths and small conducting vessels, the diaphragm bundles are mainly composed of conducting elements only surrounded by a thin layer of sclerenchyma tissues. Above the node, many small tangential vascular bundles that turn and twist forming a ring around the culm can be detected; an observation that agrees with previous observations by [1][11][12]. Thin fibers developing radially can also be observed above the diaphragm of the node (Fig. 3 and 5, white arrows) that originate by branching from the main longitudinal fibers. Above the node, the combination of radial, tangential and longitudinal bundles creates a three-dimensional

 

interwoven net of fibers [9][14]. When moving away from the node, the longitudinal fibers regain their original elongated shape and lateral sheaths appear again.

An automatic segmentation of the sample was also performed, enabling the visualization of the global pattern of vascular bundles (fibers and conducting vessels) in the node (Fig. 6). The ring of tangential and radial fibers above the node can be well identified on Fig.6a., and the pattern of "splitting bundles" joining the diaphragm from the inner side of the culm can be noticed on Fig.6b. Concerning the conducting vessels, Figs.6c. and 6d. show that they remain mostly longitudinal, except near the diaphragm where tangential vessels appear in the inner side of the culm, as well as vessels crossing horizontally the diaphragm. In general, a high connectivity between the vascular bundles can be observed especially in the diaphragm and in the inner layer of the culm, which is consistent with the findings of [14] and [7], who first noticed that an "intensive fusion and re-separation" of vascular bundles occurs in the node. Through the fusion of vascular bundles in the diaphragm, most conducting vessels can cross from one side of the culm to the other, as is shown in Figure 6d.

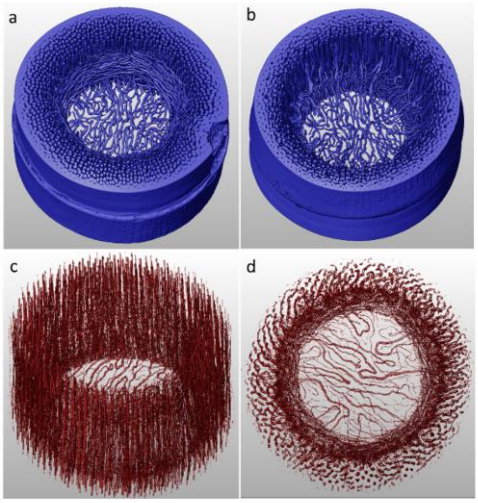


*Figure 6. (a) Segmentation of the fibers, top side view. (b) Segmentation of the fibers, bottom side view. (c) Segmentation of the conducting vessels, top side view. (d)*

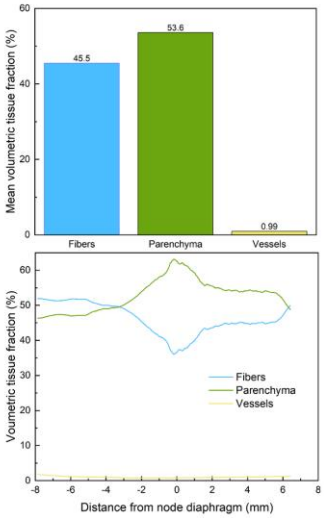


*Figure 7. (top) Mean tissue fractions over the whole sample. (bottom) Distribution across the node.*

Using this segmentation, the volumetric fraction of fibers, vessels and parenchyma could directly be computed at different positions of the culm (Fig. 7). The mean volumetric fractions over the whole node were also computed: the sample is composed of 53.6% parenchyma, 45.5% fibers and 0.99% conducting vessels. Those fractions differ quite significantly from what had been found by [14], who reported a smaller content of fibers and larger amount of conducting vessels. This discrepancy could however be explained by the different species of bamboo used as well as the uncertainty of measurement due to the segmentation. The profile of fiber content across the node seems however to corroborate the trend observed by [14]. Starting from below the node, the fiber content decreases as the culm thickens and reaches a minimum of 36% at the location of the diaphragm. Above the node, where the ring of tangential bundles is present and the culm remains thick, the fiber content stagnates at 45%, before regaining its internodal value of about 51%. This shows that for *Arundinaria amabilis bamboos*, nodes have a lower fiber

 

content than internodes, despite the apparition of horizontal bundles and the coarser fibers in the node.

The X-ray microtomography that was performed in the frame of this work allowed the detailed analysis of the morphology of an *Arundinaria amabilis* bamboo node. Specific characteristics of the node were identified and clearly visualized for the first time, such as the splitting bundles, the diaphragm structure, and the interwoven net of tangential, radial and longitudinal bundles above the diaphragm. From a biological perspective, this analysis confirms the important role of the node for the transport of water and nutrients [1]: the splitting bundles as well as the high connectivity of the vascular bundles in the diaphragm allow water and nutrients to be transported along the whole culm, longitudinally as well as transversely. Concerning the mechanical properties of the node however, it is hard to reach conclusions based solely on this morphological analysis. On the one hand, the deviations undergone by the longitudinal fibers and especially the splitting bundles, combined with the low fiber content of the node, could be an indicator for the weakness of the node and its low tensile strength [15, 16]. On the other hand, the interweaving fibers above the diaphragm could strengthen the node and make it more resistant to crack propagation [9]. In this context, using µCT to build a finite-element model of the node to perform numerical simulations could be particularly interesting.

### 3.2 Finite element discretization

The building of a finite-element model of the node based on the segmentation of the µCT image stack was attempted. To simplify the complex geometry of the node, only the fibers and the parenchyma were segmented and considered for the creation of the mesh. It was chosen to neglect the conducting vessels since they only make up a few percent of the total volume of the node. As mentioned in the introduction, [4] and [13] already succeeded in meshing respectively a small internode sample of 2x2 mm and a branching node of about 2 mm in diameter and 8 mm in height.

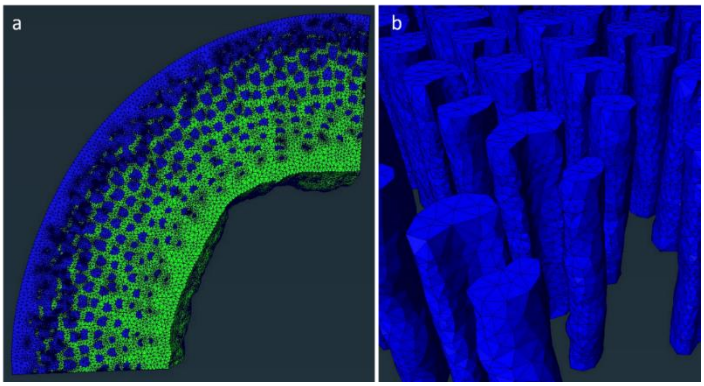


*Figure 8. Finite-element model of a part of the culm using the X-Wind module of AVIZO 3D. (a) Meshed sample. Parenchyma in green and fibers in blue. (b) Close-up of the fibers' mesh.*

However, the structure of the node investigated in this work is very different from the structure analyzed by Palombini et al. and its size is much bigger (an order of magnitude). Therefore, the manual segmentation method used by Palombini et al., which, although it is very time consuming, allows a clean segmentation and a relatively easy meshing, could not be used in this case. An attempt was therefore made at finding a way to build a mesh of the node using only an automatic threshold segmentation of the fibers.

 

Several difficulties were encountered. Initially, to obtain a clean segmentation of the fibers, the µCT images need to be well contrasted and the level of contrast should be uniform over the whole sample. Also, a high resolution is required, which can be a limitation when the scanned sample is big. For example, in this case, the fibers located on the outer side of the culm could not be segmented separately because of a lack of resolution. Finally, due to the complexity of the structure around and in the node, with thin fibers that merge and separate randomly, the resulting surfaces are complicated and make the computation of the mesh very heavy and prone to errors.

Since the meshing of the node proved difficult, an attempt was made at modeling a simpler and smaller part of the culm located above the node, were most of the fibers are oriented longitudinally. The sample considered consists of a quarter of the culm (diameter of 27 mm) of height 1.43 mm. The segmentation was made with an automatic threshold. As mentioned in Section 2.4, two approaches were followed to obtain a good meshing of the structure. The first approach consists of triangulating the surface of the structure using the "Generate surface" function of AVIZO 3D and exporting the resulting surface mesh to Meshmixer for repairing and remeshing operations. Using this repaired and remeshed surface, the final 3D finite-element model can be built using Gmsh. However, this method is not optimal, due to the complication of using different interfaces and the difficulty of repairing the errors generated when creating the surface mesh with AVIZO 3D. The second approach used the X-Wind meshing module of AVIZO 3D, which automatically builds the 3D mesh based on the provided segmentation without having to first create a triangulated surface. This approach resulted in a mesh composed of about 1’400’000 tetrahedrons for both the parenchyma and sclerenchyma (Fig. 8), which remains a reasonable number from a computational point of view while allowing to retain enough details regarding the geometry of the structure. This second approach proved to be efficient and more straightforward than the first one.

Using an automatic threshold segmentation of a µCT scan, a finite-element model for a relatively big internode sample of the culm has been built here. However, the more complex structure of the fibers in the node could not be modeled using this simple procedure since the computation of the mesh quickly became too heavy. Such a model would indeed require a higher scanning resolution as well as a relatively clean segmentation of the fibers, thus avoiding the need to mesh overly complex surfaces.

## Conclusions

This study aimed at better understanding the morphological structure of a bamboo node using X-ray microtomography, focusing on investigating the influence of the vascular bundles' layout in the node on the node's mechanical properties. In this context, the potential of µCT for building a finite-element model of the node was also explored. Specific characteristics of the node were identified and clearly visualized for the first time, such as the "splitting bundles", the diaphragm structure and the interwoven net of tangential, radial, and longitudinal bundles above the diaphragm.

From a biological point of view, the existence of splitting bundles and the high connectivity of the vascular elements in the diaphragm seem to indicate that one of the primary roles of bamboo nodes is to allow the transverse transportation of water and nutrients in the culm. Regarding the node's mechanical performance however, the deviations undergone by the longitudinal fibers as well as the low fiber content in the node might indicate that nodes are

 

weak points in a bamboo culm, in line with the findings of [15][16]. The net of interweaved bundles identified above the node could in this case be viewed as an attempt to reinforce a weak but essential component of the bamboo culm, since it has been show that the net-like pattern of the node increases its fracture toughness [16].

This study also showed that if the µCT technique has a great potential for meshing large portions of the culm, it reaches its limitations when attempting to mesh more complex structures such as the center of the node, based on a simple threshold segmentation. Once a way to model the node is found, a combination of finite-element analysis and mechanical tests could help conclude on the mechanical strength and properties of bamboo nodes.

## Acknowledgements

We thank Gary Perrenoud for micro-CT measurements at the EPFL Platform for X-Ray Radioscopy and Tomography (PIXE). This work was supported through an ENAC Exploratory grant 2018/2020 in the frame of the “New plant-based composite materials” project.

## 1. References

1. Liese, W. (1998). The anatomy of bamboo culms, volume 18. Brill.
2. Amada, S., Munekata, T., Nagase, et al. (1996). The mechanical structures of bamboos in viewpoint of functionally gradient and composite materials. J Comp Mat, 30(7):800–819.
3. Dixon, P. G. and Gibson, L. J. (2014). The structure and mechanics of moso bamboo material. Journal of the Royal Society Interface, 11(99):20140321.
4. Palombini, F. L., et al. (2016). Bionics and design: 3d microstructural characterization and numerical analysis of bamboo based on x-ray microtomography. Mat Char, 120:357–368.
5. Obataya, E., et al. (2007). Bending characteristics of bamboo (phyllostachys pubescens) with respect to its fiber–foam composite structure. Wood sci technol, 41(5):385–400.
6. Lee, C. et al. (1960). Anatomical studies of some chinese bamboos. J Integ Plant Biol, 9(1).
7. Grosser, D. and Liese, W. (1971). On the anatomy of asian bamboos, with special reference to their vascular bundles. Wood Science and technology, 5(4):290–312.
8. Ding, Y. and Liese, W. (1995). On the nodal structure of bamboo. Bamboo Res, 14:24–32.
9. Chen, G. and Luo, H. (2020). Effects of node with discontinuous hierarchical fibers on the tensile fracture behaviors of natural bamboo. Sust Mat Technol, 26:e00228.
10. Huang, P., Chang, W.-S., Ansell, M. P., et al. (2015). Density distribution profile for internodes and nodes of phyllostachys edulis (moso bamboo) by computer tomography scanning. Construction and Building Materials, 93:197–204.
11. Peng, G., Jiang, Z., Fei, B., et al. (2014). Detection of complex vascular system in bamboo node by x-ray µct imaging technique. Holzforschung, 68(2):223–227.
12. Xiang, E., Yang, S., Cao, et al. (2021). Visualizing complex anatomical structure in bamboo nodes based on x-ray microtomography. J. Renew Mater, 9(9):1531.
13. Palombini, F. L., Nogueira, F. M., Kindlein, W., et al. (2020). Biomimetic systems and design in the 3d characterization of the complex vascular system of bamboo node based on x-ray microtomography and finite element analysis. Journal of Materials Research, 35(8):842–854.
14. Li, S., Yang, S., Shang, L., Liu, X., et al. (2021). 3d visualization of bamboo node’s vascular bundle. Forests, 12(12):1799.
15. Shao, Z., Zhou, L., Liu, Y., et al. (2010). Differences in structure and strength between internode and node sections of moso bamboo. J of Tropical Forest Science, pages 133–138.
16. Taylor, D., Kinane, B., Sweeney, C., et al. (2015). The biomechanics of bamboo: investigating the role of the nodes. Wood science and technology, 49(2):345–357.

 